Effect of an impurity in a quantum resonator

Y. Takagaki and D. K. Ferry
Center for Solid State Electronics Research, Arizona State University, Tempe, Arizona 85287-6206
(Received 26 August 1991)

We present a numerical study of the influence of disorder on quantum-mechanical transmission by considering the presence of an impurity in a T-shaped quantum-wire junction. The device is modeled as an electron waveguide of finite cross section. Transmission and reflection probabilities are computed by use of a waveguide-matching technique. The calculations show that the transmission of the two-dimensional electron gas through the narrow-wide-narrow geometry can be both enhanced and suppressed by the presence of a repulsive impurity potential. Although perfect transparency is not generally achieved with the presence of a single impurity, we find a 100% modulation of conductance as one device parameter is changed, which is robust against the scattering. If the impurity is located in the narrow-wire region, a periodic oscillation appears in transmission due to multiple reflections between the impurity and the stub region. We also examine an attractive scatterer.

As a result of advances in microfabrication technology, it has become possible to observe quantum interference phenomena in semiconductor microstructures.[1,2] In mesoscopic systems, where the phase coherence length L_ϕ is larger than the sample size, the wave nature of an electron needs to be taken into account. The conductance of a device can be modulated by changing the phase of an electron wave instead of the amplitude. The phase of the electron wave can be modified by changing the energy or by applying a magnetic field. Universal conductance fluctuations,[3] the Aharonov-Bohm effect,[2,4] and nonlocal effects[5] in electronic transport are clear manifestations of this regime which cannot be described by classical transport theory. Recently, interest has been raised in ballistic-transport properties of narrow channels. In highly purified semiconductor materials, the elastic mean free path l_e of an electron can be over 10 μm and, hence, the electron motion is ballistic. The electron wavelength in semiconductors is longer than in metals and may be comparable to the size of the sample. Hence, semiconductor quantum wires can be viewed as electron waveguides.[6] In this regime, one can expect the analogs of microwave or optical waveguides in semiconductor nanostructures.[7] A transistor action directly based on the modulation by quantum-mechanical effect has been proposed in the last few years.[8,9] In small disordered wires, the amplitude of the conductance fluctuations is on the order of e^2/h and, thus, $\sim 0.1\%$ in metals and $\sim 10\%$ in semiconductors.[10] On the other hand, nearly 100% modulation may be possible in the ballistic regime.[8] This is a great advantage for device applications since a large change in the transmission can be induced by a small change in a sample parameter.

If there are no impurities within the device, resistance arises only by scattering from geometrical features such as an abrupt change in the width of the channel or a junction with external leads. However, we have to be careful in the analysis to consider the inevitable presence of crystal defects, residual impurities, and nonspecular boundary scattering in real devices.[11] Since mesa fabrication by use of ion-beam etching is one of the most used techniques to delineate quantum structures, we can say that the smaller the sample dimensions the more plausible the presence of process-induced defects in the conduction channel. The conductance of the phase-coherent structure has been recognized to be sensitive to an individual impurity even if it is outside of the classical current path.[12] Gigantic quantum-mechanical oscillations of the bend resistance R_B predicted in a rounded cross[13,14] are suppressed by impurities. Experiments on R_B suggest that we cannot avoid the scatterings from impurities even if the sample dimensions are more than two orders of magnitude smaller than l_e. Agreement between the experimental observation and the numerical results can be obtained by including some impurities in the calculation.[13,15] The effect of sample imperfections on the conductance quantization phenomena in a narrow constriction, wide-narrow-wide (W-N-W) geometry, has been calculated previously.[16,17] The conductance of a ballistic-point contact shows steps of $2e^2/h$ as the constriction is widened.[18] The quantization is strongly distorted by impurities in the orifice region and the plateaus disappear as the scatterer gets strong.[16,17]

In this paper, we investigate the influence of the scattering from a single δ-function impurity on transmission properties of a quantum resonator. We consider a three-port quantum transistor (N-W-N geometry) in which one port is used as a remote gate to control the transmission. The current in the device is controlled by changing the boundary conditions, i.e., the length of the stub region. The device was proposed by Datta[8] and Sols *et al.*[9] We present numerical results to illustrate the variations of the interference pattern caused by the consideration of an impurity.

Consider a quantum-mechanical motion of a noninteracting electron with Fermi energy $E_F=\hbar^2 k_F^2/2m$ in the T-shaped resonator shown in Fig. 1. The waveguide consists of a wide strip defined by $(-a>x$

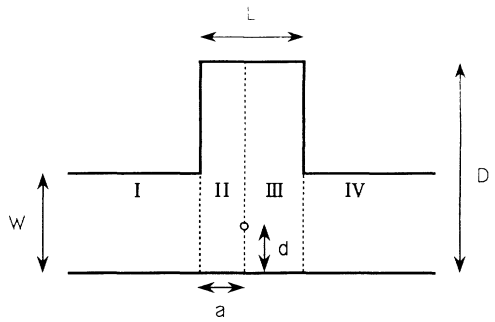

FIG. 1. Schematic of a T-shaped electron waveguide. A single δ-function impurity is placed in the stub region. We assume hard-wall square-well confinement. The transmission and reflection probabilities are obtained by matching the wave function at the boundaries $x=-a$, 0, and $L-a$.

$<L-a, 0<y<D$) and two narrow semi-infinite strips defined by $(-\infty<x<-a, 0<y<W)$ and $(L-a<x<\infty, 0<y<W)$, which are connected to two reservoirs at each end. We ignore inelastic scattering throughout the device. Suppose the electron incident from left in channel n is transmitted to channel m in the right-hand side strip with the probability of T_{mn} or reflected to channel m in the left-hand side strip with the probability of R_{mn}. The two-terminal conductance, which is the ratio of the transmitted current to the potential difference between two reservoirs, is evaluated using the linear conductance formula[19]

$$G=\frac{2e^2}{h}\sum_{m,n}T_{mn}\ , \tag{1}$$

where the sum runs over the propagating modes of the wire, since evanescent modes do not contribute to the current in an infinite channel. In the absence of impurities the transmission probabilities can be estimated by matching the wave function and the derivative at the N-W boundaries $x=-a$ and $x=L-a$.[14]

Consider now a single δ-function potential sited at $x=0$:

$$V_i(x,y)=\gamma\delta(x)\delta(y-d)\ . \tag{2}$$

If the screening length is comparable to the wavelength, such as the case in GaAs-$Al_xGa_{1-x}As$, the long-range nature of the scattering potential[20] may need to be taken into account. However, the essential features will be described within an assumption of a short-range scatterer. The Hamiltonian in the effective-mass approximation is

$$H=\frac{p_x^2+p_y^2}{2m}+V_c(y)+V_i(x,y)\ , \tag{3}$$

where $V_c(y)$ represents a confining potential. Throughout this paper we assume hard-wall confinement along the guide aide walls, for simplicity. In order to evaluate the transmission coefficients, we have to consider the wave-matching problem at $x=0$.[21] The wave function in the regions II $(-a<x<0)$ and III $(0<x<L-a)$, where the scattering potential is zero, can be given as an expansion in standing waves of the form

$$\Psi=\sum_j\chi_j(y)u_j(x)\ , \tag{4}$$

$$\sum_j\sqrt{2/D}\sin\left[\frac{j\pi}{D}y\right](A_je^{iq_jx}+B_je^{-iq_jx}),\quad -a<x<0\ , \tag{5a}$$

$$\sum_j\sqrt{2/D}\sin\left[\frac{j\pi}{D}y\right](C_je^{iq_jx}+D_je^{iq_jx})\ ,\quad 0<x<L-a\ . \tag{5b}$$

The sum over j includes evanescent modes for which the wave vector q_j of the mode j is imaginary, and so we have

$$q_j=\sqrt{k_F^2-(j\pi/D)^2} \tag{6a}$$

for propagating modes $(j\pi/D<k_F)$ and

$$q_j=i\sqrt{(j\pi/D)^2-k_F^2} \tag{6b}$$

for evanescent modes $(j\pi/D>k_F)$. In the presence of a scatterer, each mode in region II couples with all modes in region III. Using the orthogonality property of the sinusoidal functions $\chi_j(y)$, we obtain from the Hamiltonian Eq. (3)

$$\frac{d^2u_j(x)}{dx^2}+q_j^2u_j(x)=\sum_m\gamma_{jm}(x)u_m(x)\ , \tag{7}$$

where

$$\gamma_{jm}(x)=\frac{2m}{\hbar^2}\int\chi_j(y)V_i(x,y)\chi_m(y)dy \tag{8}$$

are the mode-coupling constants. Integrating Eq. (7) once gives the boundary condition for the derivative of wave function[21]

$$\left.\frac{du_j(x)}{dx}\right|_{x=0^+}-\left.\frac{du_j(x)}{dx}\right|_{x=0^-}=\sum_m\Gamma_{jm}u_m(0)\ , \tag{9}$$

where

$$\Gamma_{jm}=\frac{4m\gamma}{\hbar^2D}\sin\left[\frac{j\pi d}{D}\right]\sin\left[\frac{m\pi d}{D}\right]\ . \tag{10}$$

Mode coupling is crucial when the magnitude of the wave function is maximum at the position of an impurity. Substituting Eq. (5), we have

$$iq_j(C_j-D_j)-iq_j(A_j-B_j)=\sum_m\Gamma_{jm}(A_m+B_m)\ . \tag{11}$$

The continuity of the wave function requires

$$A_j+B_j=C_j+D_j\ . \tag{12}$$

We have solved for the transmitted and reflected wave amplitudes using Eqs. (11) and (12) and the matching equations at $x=-a$ and $x=L-a$. We note that, as discussed by Sols *et al.*,[9] $L/W\sim1$ and a single-mode regime are desirable for transistor operation. In the following calculations we take, unless otherwise noted, the size of the stub to be $L/W=1.0$ and $D/W=1.6$ and the num-

ber of incident modes to be less than two.

In Fig. 2, the conductance is shown as a function of $k_F W/\pi$, which counts the total number of occupied channels in the wire, for a repulsive scatterer having strength $U=4m\gamma W/\hbar^2 D$. If we take $W=10$ nm and the mass of the electron to be the effective mass for GaAs $m=0.067m_0$, we have $\gamma/W^2=4.55U$ meV. The size of the stub D/W is 1.6 in Fig. 2(a) and 2.1 in Fig. 2(b). The solid line represents an impurity-free interference pattern. The dips in the conductance move lower in energy and the number increases with increasing D/W.[9] These dips are due to interference of two paths, one of which is directly transmitted from left to right, and the other one is transmitted after reflections in the stub region.[8] As the scatterer is strengthened, the transmission becomes transparent for the energies below the first dip while opaque when the energy is between the dip and the threshold for propagation in the second transverse mode. It may be noteworthy that a repulsive impurity inside the constriction always reduces the conductance for a point contact structure (W-N-W configuration), while one outside the constriction can both enhance or suppress the conductance.[16]

Figure 3 shows the dependence of the conductance on the position of an impurity. As we will show below, the conductance does not change as the repulsive scatterer is

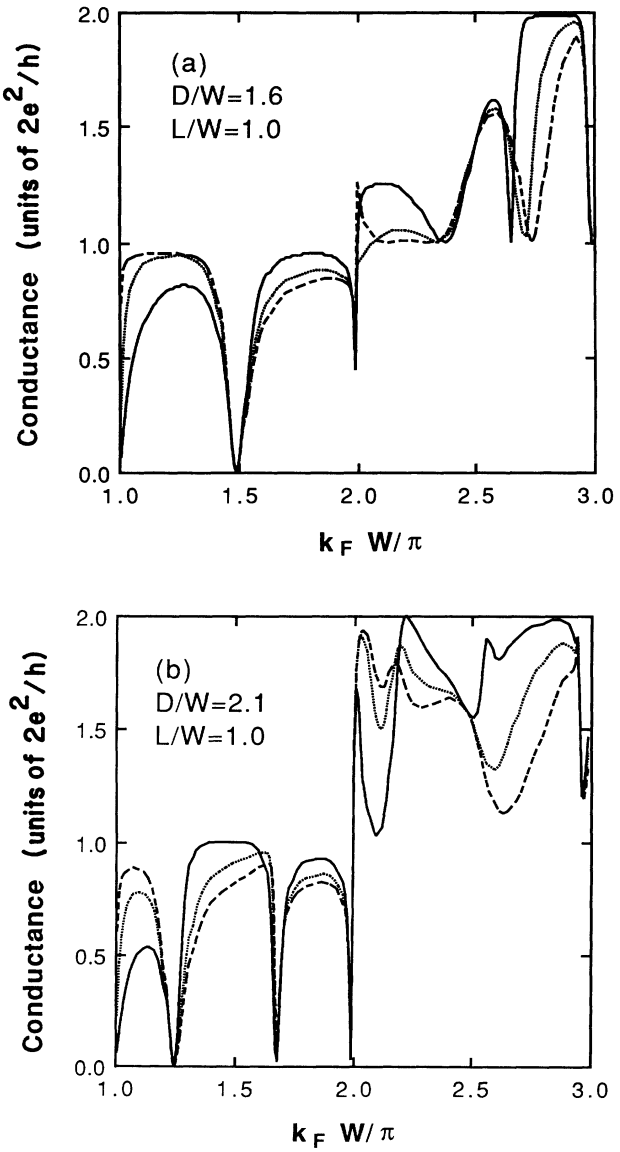

FIG. 2. Two-terminal conductance for a repulsive impurity in the stub region with $a/W=0.57$ and $d/W=0.68$. The solid, dotted, and dashed lines represent the conductance for $U=0$, 5, and 50, respectively. Device dimensions are (a) $D/W=1.6$ and $L/W=1.0$ and (b) $D/W=2.1$ and $L/W=1.0$.

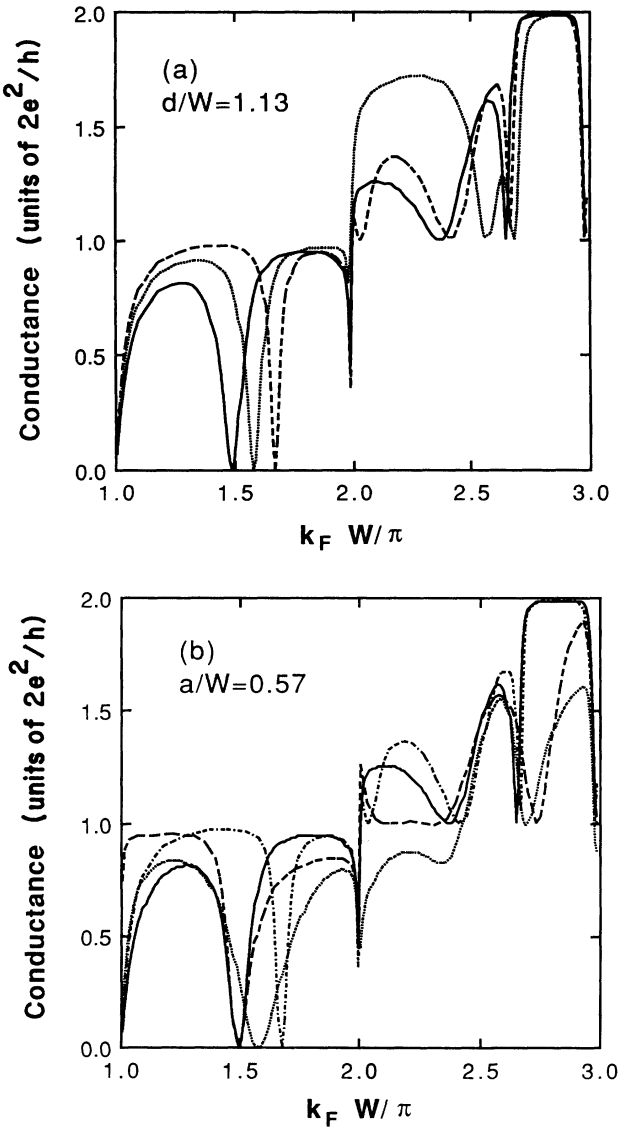

FIG. 3. Two-terminal conductance as a function of $k_F W/\pi$ for various positions of an impurity with the strength of $U=50$. For the repulsive scatterer dips move higher in energy. The solid lines are conductance in the absence of an impurity. (a) The impurity is moved along the x axis with $d/W=1.13$. For dotted and dashed lines a/W is 0.26 and 0.43, respectively. (b) The impurity is moved along the y axis with $a/W=0.57$. The dotted, dashed, and dash-dotted lines show conductance for $d/W=0.32$, 0.68, and 1.13, respectively.

made sufficiently strong, so that we consider a relatively strong potential to avoid a dependence on U. The impurity is moved along the x axis in Fig. 3(a) with $d/W=1.13$, and along the y axis ($a/W=0.57$) in Fig. 3(b). Note that the dips shift in energy depending on the location of an impurity, but the nearly total reflection still occurs. The probability distribution of wave function at the dip ($k_F W/\pi \approx 1.5$) plotted in Fig. 4 shows two peaks of probability inside the stub region. One can see that the dips are insensitive to the impurity placed at the node of the wave function ($y/W \sim 0.6$–0.8). On the other hand, the dip moves higher in energy if the impurity is put at the peaks of the probability as shown in Fig. 3(b). The transmission property becomes independent of U for large U, since the wave function vanishes at the position of the repulsive impurity. Increasing the number of incident channels causes the interference pattern to become aperiodic and, thus, the effect of the impurity is not straightforward. However, one can see similar tendency.

In Fig. 5, the two-terminal conductance is plotted as a function of D/W for $k_F W/\pi=1.6$. In the absence of an impurity, the conductance reveals a periodic pattern of 100% modulation between perfect transparency and perfect opaqueness. The period is exactly $\lambda/2$, where λ is the wavelength of the incident electron.[9] If an impurity is put in the stub region, we observe, in general, that (1) maximum conductance is suppressed, (2) the dips occur at larger D/W, and (3) the dips are not necessarily evenly spaced and the period is slightly larger than $\lambda/2$.

In contrast to a repulsive potential, an attractive potential induces quasibound states which split off from one of the evanescent modes. We show in Fig. 6 the conductance for an attractive δ-function potential. The quantum interference pattern is affected even when the potential is relatively weak. In Fig. 6(a), the impurity is located at the same position as Fig. 3(a), i.e., the node of the wave function at the resonance. Here again the dip at $k_F W/\pi \approx 1.5$ is almost independent of the impurity. We observe that the standing wave pattern of the wave function corresponding to the dip is robust against this impurity. The probability at the position of the impurity remains almost zero even if the potential is made more attractive. The conductance of the attractive scatterer is increased or decreased, depending on the strength of potential. For an attractive scatterer the conductance can be much smaller. With increasing strength, the conductance decreases and nearly total reflection occurs over a wide range of energy when $U \sim -5$. Bagwell observed the overall decrease of the conductance in a quasi-one-dimensional wire with an attractive impurity and has discussed this in terms of the transmission resonances due to quasibound states which move lower in energy as the scatterer is made more attractive.[21] The conductance increases if the quasi-bound-state energy has moved below the subband minimum as the strength of the scatterer is further increased. Figure 6(b) shows the conductance through an impurity with $d/W=1.13$. Interestingly, for this impurity, the overall decrease of the conductance is not observed. If an impurity potential is repulsive, its effect is always to move dips to higher energy. On the other hand, an attractive potential moves the resonance energies lower, reflecting the presence of the quasibound states. The dips disappear when the energy aligns with the bottom of the subbands. Additional narrow dips, corresponding to the quasibound states, appear immediately below each subband threshold and move lower in energy as the potential is made more attractive.

Next, we place an impurity in the narrow wire (region I). We now have a parameter b, which represents the distance along the x direction between the impurity and the interface between regions I and II. We have calculated D/W dependence of the conductance for fixed energies. We find that the dips are not affected by the impurity in

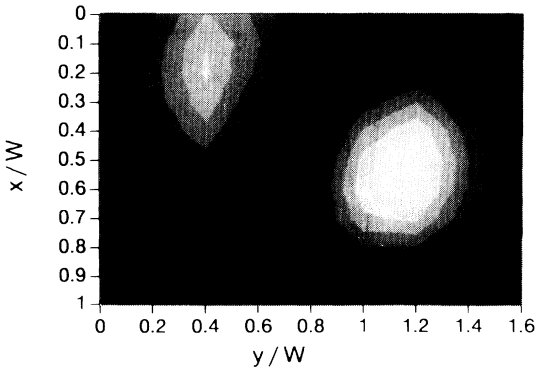

FIG. 4. Probability distribution of wave function in the stub region with $k_F W/\pi \approx 1.5$. The brighter the reflection, the larger the probability. We consider a perfect waveguide with the dimensions $D/W=1.6$ and $L/W=1.0$. The stub region shown is connected to two semi-infinite wires ($0<y/W<1$) at $x/W=0$ and $x/W=1$. The electron moving in the positive direction of the x axis with this energy is perfectly reflected in the stub region.

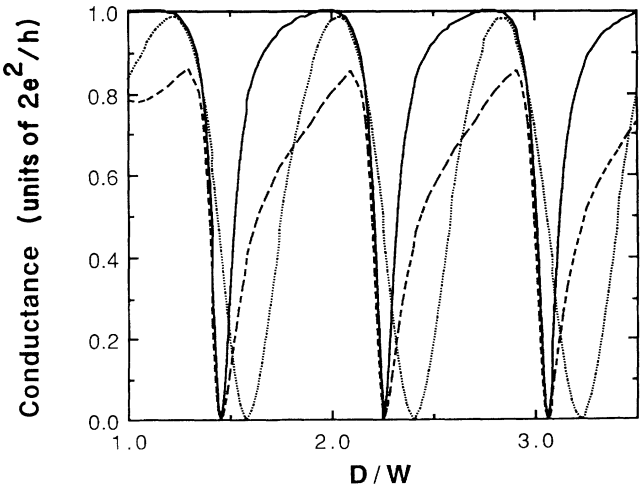

FIG. 5. Two-terminal conductance as a function of D/W for $k_F W/\pi=1.6$. In the absence of an impurity (solid line), the period corresponds to one-half of the wavelength of the incident electron. The period is slightly increased if an impurity ($a/W=0.4$, $d/W=0.4$, $U=50$) is put in the stub region (dotted line). For the dashed line an impurity is put in the narrow wire region ($b/W=0.4$, $d/W=0.54$, $U=50$).

the wire as shown by the dashed line in Fig. 5. The only effect is to suppress the maximum of the conductance. The conductance is no longer unity if there is an impurity. In Fig. 7(a) the conductance is plotted as a function of $k_F W/\pi$. One can see an oscillation due to successive resonances between the δ-function barrier and the stub resonator.[22] The b/W dependence of the conductance also reveals the oscillation and the period corresponds to integer multiples of one-half of the wavelength. For $k_F W/\pi > 2$ the oscillation shows beat structure, since two propagating modes, which have different wavelengths, are available in the wire. The oscillation also occurs for an attractive scatterer as shown in Fig. 7(b). The conductance again shows an overall decrease when $U \sim -5$. This is still observed even if $D/W = 1$, indicating that this behavior arises from the presence of an attractive impurity in a quasi-one-dimensional wire.

In conclusion, we have considered the electron

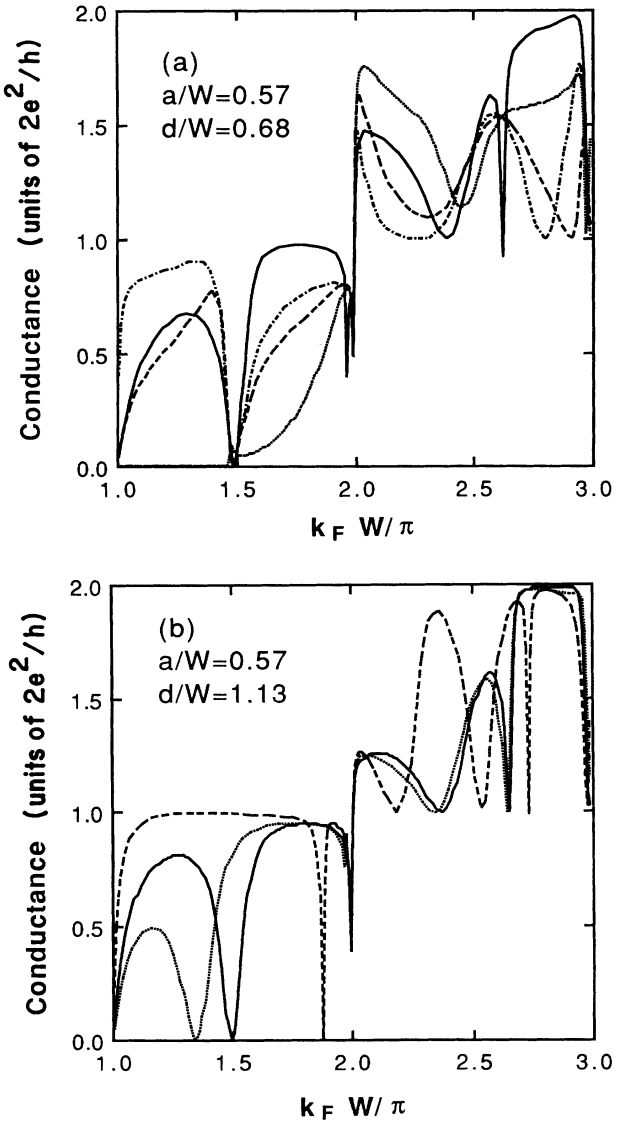

FIG. 6. Two-terminal conductance for an attractive δ-function impurity in the stub region. (a) The solid, dotted, dashed, and dash-dotted lines: $U = -1$, -3, -5, and -10, respectively. The impurity is located at $a/W = 0.57$ and $d/W = 0.68$. Nearly total reflection is observed over a wide range of energy if $U \sim -5$. (b) The dotted and dashed lines are conductance for $U = -1$ and -3, respectively. The impurity is located at $a/W = 0.57$ and $d/W = 1.13$. For this location the resonance results in narrow dips. The solid line is the conductance of a perfect electron waveguide.

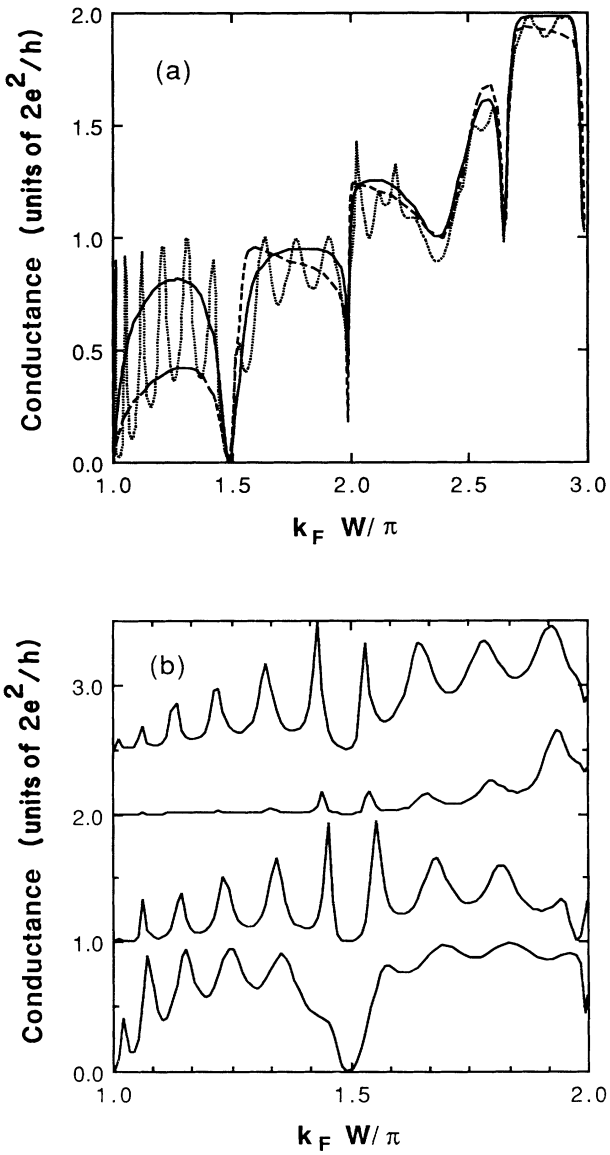

FIG. 7. Oscillation due to multiple reflections occurs if an impurity is located in the wire region. (a) Dotted line shows two-terminal conductance through a single repulsive scatterer in the wire with $b/W = 5.3$ and $d/W = 0.58$. For the dashed line the impurity is located at the interface between regions I and II ($b = 0$) with $d/W = 0.58$. The strength of the potential considered is $U = 15$. The solid line shows the conductance of a perfect electron waveguide. (b) Conductance calculated for an attractive scatterer in the wire. The strength of the potential considered is -1, -3, -5, and -10 from the bottom to the top. For clarity, curves for $U = -3$, -5, and -10, are offset by e^2/h, $2e^2/h$, and $2.5e^2/h$, respectively. Overall decrease of the conductance occurs when $U \sim -5$.

transmission through a T-shaped quantum resonator containing a single δ-function impurity. The effect of the impurity on coherent electron transmission is to increase or decrease the conductance. Almost complete transmission is destroyed, while the opaqueness at dips is stable against a single δ-function impurity. However, the positions of the dips are moved by the impurity. Quantum-mechanical multiple scattering between the impurity and the stub causes an oscillation in the conductance when the impurity is present in the wire. For an attractive scatterer, new dips appear, due to the presence of quasi-bound states in the channel.

The authors wish to thank Q. Li and K. Yano for helpful discussions. This work was supported by the Office of Naval Research.

[1]Y. Imry, *Directions of Condensed Matter Physics,* edited by G. Grinstein and E. Mazenko (World Scientific, Singapore, 1986), p. 101.

[2]S. Washburn and R. A. Webb, Adv. Phys. **35**, 375 (1986).

[3]W. J. Skocpol, P. M. Mankiewich, R. E. Howard, L. D. Jackel, D. M. Tennant, and A. D. Stone, Phys. Rev. Lett. **56**, 2865 (1986).

[4]K. Ishibashi, Y. Takagaki, K. Gamo, S. Namba, S. Ishida, K. Murase, Y. Aoyagi, and M. Kawabe, Solid State Commun. **64**, 573 (1987).

[5]A. Benoit, C. P. Umbach, R. B. Laibowitz, and R. A. Webb, Phys. Rev. Lett. **58**, 2343 (1987); W. J. Skocpol, P. M. Mankiewich, R. E. Howard, L. D. Jackel, D. M. Tennant, and A. D. Stone, *ibid.* **58**, 2347 (1987).

[6]G. Timp, H. U. Baranger, P. de Vegvar, J. E. Cunningham, R. E. Howard, R. Behringer, and P. M. Mankiewich, Phys. Rev. Lett. **60**, 2081 (1988).

[7]*Analogies in Optics and Microelectronics,* edited by W. van Haeringen and D. Lenstra (Kluwer, Dordrecht, 1990).

[8]S. Datta, Superlatt. Microstruct. **6**, 83 (1989).

[9]F. Sols, M. Macucci, U. Ravaioli, and K. Hess, Appl. Phys. Lett. **54**, 350 (1989); J. Appl. Phys. **66**, 3892 (1989).

[10]P. A. Lee, A. D. Stone, and H. Fukuyama, Phys. Rev. B **35**, 1039 (1987).

[11]T. J. Thornton, M. L. Roukes, A. S. Scherer, and B. P. van der Gaag, Phys. Rev. Lett. **63**, 2128 (1989); M. L. Roukes, A. Scherer, and B. P. Van der Gaag, *ibid.* **64**, 1154 (1990).

[12]K. S. Ralls, W. J. Skocpol, L. D. Jackel, R. E. Howard, L. A. Fetter, R. W. Epworth, and D. M. Tennant, Phys. Rev. Lett. **52**, 228 (1984).

[13]R. Behringer, G. Timp, H. U. Baranger, and J. E. Cunningham, Phys. Rev. Lett. **66**, 930 (1991).

[14]Y. Takagaki and D. K. Ferry, Phys. Rev. B **44**, 8399 (1991).

[15]T. Kakuta, Y. Takagaki, K. Gamo, S. Namba, S. Takaoka, and K. Murase, Phys. Rev. B **43**, 14 321 (1991).

[16]D. van der Marel and E. G. Haanappel, Phys. Rev. B **39**, 7811 (1989).

[17]C. S. Chu and R. S. Sorbello, Phys. Rev. B **40**, 5941 (1989).

[18]B. J. van Wees, H. van Houten, C. W. J. Beenakker, J. G. Williamson, L. P. Kouwenhoven, D. van der Marel, and C. T. Foxon, Phys. Rev. Lett. **60**, 848 (1988); D. A. Wharam, T. J. Thornton, R. Newbury, M. Pepper, H. Ahmed, J. E. F. Frost, D. G. Hasko, D. C. Peacock, D. A. Ritchie, and G. A. C. Jones, J. Phys. C **21**, L209 (1988).

[19]R. Landauer, IBM J. Res. Dev. **1**, 233 (1957); D. S. Fisher and P. A. Lee, Phys. Rev. B **23**, 6851 (1981).

[20]S. Das Sarma and F. Stern, Phys. Rev. B **32**, 8442 (1985).

[21]P. F. Bagwell, Phys. Rev. B **41**, 10 354 (1990).

[22]A. Kumar and P. F. Bagwell, Solid State Commun. **75**, 949 (1990).

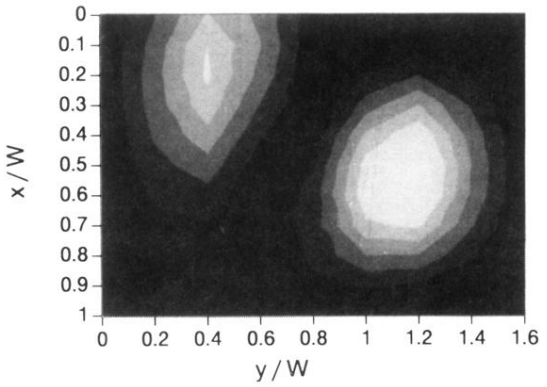

FIG. 4. Probability distribution of wave function in the stub region with $k_F W/\pi \approx 1.5$. The brighter the reflection, the larger the probability. We consider a perfect waveguide with the dimensions $D/W=1.6$ and $L/W=1.0$. The stub region shown is connected to two semi-infinite wires ($0<y/W<1$) at $x/W=0$ and $x/W=1$. The electron moving in the positive direction of the x axis with this energy is perfectly reflected in the stub region.